IJISET - International Journal of Innovative Science, Engineering & Technology, Vol. 2 Issue 5, May 2015.
www.ijiset.com
ISSN 2348 – 7968

CFD Design Enhancement of a Material Preheated Sampler Probe under an Erosion Approach

Héctor López-Aguilar[1],Jorge Gómez[2], Marco Merino-Rodarte[1], Alberto Duarte-Moller[1] and Antonino Pérez-Hernández[1]

[1] Centro de Investigación en Materiales Avanzados (CIMAV), Chihuahua, Chihuahua, México, 31109/Miguel de Cervantes 120, Chihuahua, Chihuahua, México

2 Department of physics and mathematics/ Universidad Autonoma de Ciudad Juárez (UACJ), Ciudad Juárez, Chihuahua, México, 32310/ Ave. Del charro #610 norte Fracc. Universidad, Ciudad Juárez, Chihuahua, México

Abstract

This paper presents a new design and modeling of a sampling probe with erosion particle damage perspective using the Computational Fluid Dynamic (CFD) technique. The selection of materials for the device, must resist determine heat transfer rate in certain areas and abrasive erosion occasioned for friction between the micro particles specimens in the internal walls moving at high velocities. Following earlier work, the sampling device is redesigned and a comparison is made from erosion perspective. Differences were found in the internal behavior of fluids depending on the position in which gas is injected it can be detected thought CFD analysis.

Keywords: *CFD*, erosion, oxidative damage, sample probe

1. Introduction

Any design in which have involved the concepts like jet flow and entrainment of particles inside a duct must consider the erosion effect for proper materials selection. Several Computational Fluid Dynamics (CFD) studies on the analysis of flow turbines have been done [1,2], including the analysis of turbulent flows [3]. Song et al. [4] performed the analysis of a jet type pump and Yimer et al. [5] realized a CFD model which principle of operation is based on the Venturi effect [6]. In cement industry, CFD has been used for the design and optimization of calcinators [7] and to simulate the main transport processes in rotary kilns [8].

A jet type operation is subjected to friction erosion between the fluid and the surface models that have been developed to study this phenomenon [9]. Kumar and Shukla [10] used a finite element simulation to determine the crater of a particle which impacts a surface. Also Graham et al. [11] study the erosion caused by high velocity fluid trough CFD analysis.

In cement industry, a qualitative and quantitative control method of the samples taken prior at the pre-calciner, that is before the material enters to the rotary kiln, and at end-product are necessary to ensure the quality of clinker. For this task a sampler probe was developed, the samples are found at a high temperature and under an atmosphere of CO_2, which are susceptible to oxidation in air. In previous work, a sampler probe was design with ANSYS CFD software. A preliminary geometrical shape device was obtained from design of experiments and response surface modeling [12,13]. The objective of the current study was to identify the potential behavior of erosion rate in the system wall and evaluate the best option between two sampling probe designs through the use of CFD erosion approach.

2. Methods

2.1 Computational approach

The gas flow was modeled inside the extraction probe chamber employing the finite volume Ansys-Fluent 15.1 software [14].

In this device a 300 MPa pressure gas stream was injected perpendicularly to the extraction pipe, where creates negative pressure used in the specimen extraction. Also, a tangential cold gas stream for 500 MPa was injected in order to induce a swirl phenomenon in the chamber probe. This action extends the residence time and completes the particles cooling.

The new designs are focused on minimizing the erosion effect in order to preserve the structure in present phases through a quick cooling in a protective atmosphere. The extreme conditions inside the cyclone are ≈1090 K on rich CO_2 atmosphere.

ISSN 2348 – 7968

The considered conditions for this simulation were:

- Turbulent phenomenon flow.
- Continuous phase flow coupling with a discrete phase in steady state was considered.
- The wall inside the device was considered adiabatic.

2.2 Computational solution domain

Two computational model domain created in ANSYS Design Modeler is shown in Fig. 1. The first model has a secondary injection of cold air into the main tube, was named as Inlet Tangential in main Tube (ITT). The second model has a secondary injection of cold air into a cone, was named as Inlet Tangential in Cone (ITC).

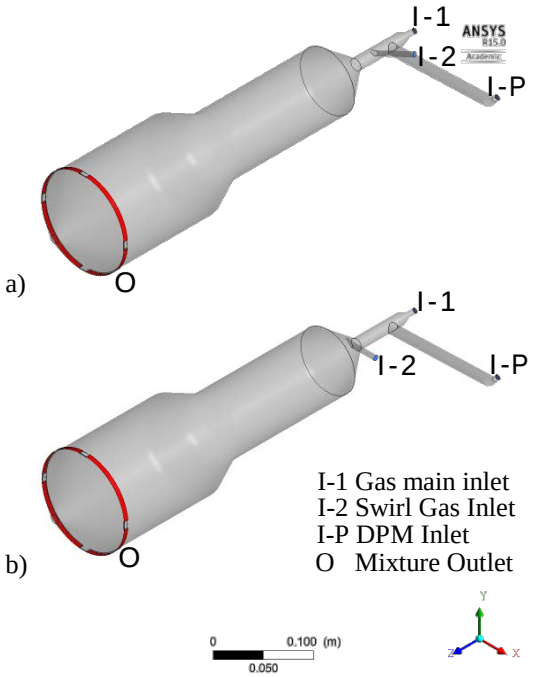

Fig. 1 Computational models a) Inlet Tangential in main Tube (ITT) and b) Inlet Tangential in Cone (ITC).

2.3 Grid Generation

The grid method in both designs was equal, were used tetrahedral cells as domain meshing and general inflation methods for the grid near to the walls. The Fig. 2a); 2b) shown the mesh for the global domain and the Fig. 2c) shown with more detail the internal mesh in a common zone. The mesh for the domain ITT has 405,035 elements and 133,332 nodes with 0.897 of average orthogonal quality and the mesh for the domain ITC has 421,569 elements and 136,263 nodes with 0.8952 of average orthogonal quality. The mesh employed determines the accuracy of the solution. Therefore, in this work a mesh quality is achieved. The convergence criteria used software allows to choose a better mesh densely elements, considering the size of the device.

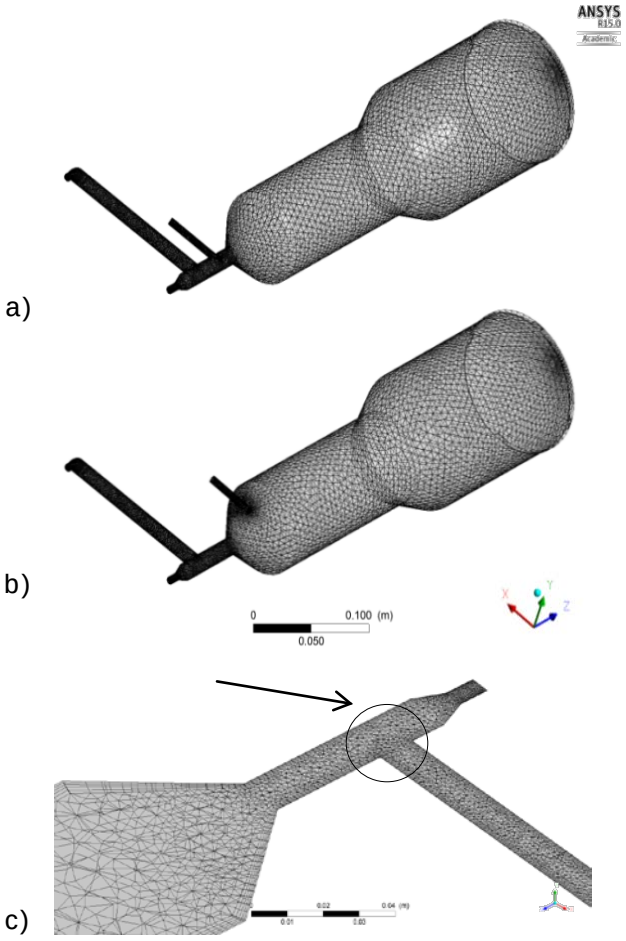

Fig. 2 Mesh computational models a) ITT, b) ITC and c) Detail of internal mesh in general zone.

2.4 Governing Fluid Flow Equations

The governing equations of continuity (1), conservation of momentum (2) and energy (3) are used to solve the flow and heat transfer of the continuous and the dispersed phase.

$$\frac{\partial \rho}{\partial t} + \nabla . (\rho \vec{v}) = S_{mass\,DPM} \quad (1)$$

ISSN 2348 – 7968

Where ρ is the density, $\vec{v}$ is the velocity magnitude, $S_{mass\ DPM}$ is the phase discrete source, p is the static pressure, $\bar{\bar{\tau}}$ is the stress tensor, and $\rho\vec{g}$ and $\vec{F}$ are the gravitational and external body forces, respectively.

$$\frac{\partial}{\partial t}.(\rho\vec{v}) + \nabla.(\rho v\vec{v}) = -\nabla p + \nabla(\bar{\bar{\tau}}) + \rho\vec{g} + \vec{F} \tag{2}$$

$$\frac{\partial}{\partial t}(\rho E + \nabla((\rho E + p)) = \nabla\left(k_{ijf}\nabla T - \sum_j h_j \vec{J}_j + (\bar{\bar{\tau}}_{ijf}\vec{v})\right) + S_h. \tag{3}$$

Where E is the total energy, k_{iif} is the effective conductivity, T is the temperature, h is the sensible enthalpy, J diffusion flux and S_h includes the heat of chemical reaction.

The first term on the right-hand side in Eq. (3) represents an energy transfer due to conduction, species discussion and viscous dissipation, respectively.

The turbulence of fluid flow was modeled by the Reynolds stress model (RSM), Eq. (4), that is an elaborate type of Reynolds-Averaged Navier Stokes by solving transport equations for the Reynolds stresses, because it cans a better prediction for turbulent flow through of seven differential and simultaneous equations [14].

$$\frac{\partial}{\partial t}(\rho\overline{u_i'u_j'}) + C_{ij} = D_{T,ij} + D_{L,ij} - P_{ij} - G_{ij} + \emptyset_{ij} - \varepsilon_{ij} - F_{ij} + S_{user} \tag{4}$$

Where the first term on the left-hand side is local time derivative, C_{ij} is the convection effect, $D_{T,ij}$is the turbulent diffusion, $D_{L,ij}$ is the molecular diffusion, P_{ij} is the stress production, G_{ij} is the buoyancy production, $\emptyset_{ij}$ is the pressure strain model (In this study the Pressure-Strain Model was considered linear), ε_{ij} is the dissipation effect, F_{ij} is the production by system rotation and S_{user} is the User-Defined Source Term.

2.5 Discrete Phase Model

The Lagrange discrete phase model (DPM) follows the Eulerian-Lagrange Approach, Eq. (5). The fluid was modeled as a continuous phase in the solution of Navier-Stokes equations, while the disperse phase was solved by tracking a large number of particles through the flow field calculated. The exchange momentum, mass and energy of the dispersed phase with the continuum phase were considered:

$$\frac{du_p}{dt} = \frac{18\mu C_D Re}{\rho_p {d_p}^2\, 24}(\vec{u} - \vec{u}_p) + \frac{\vec{g}(\rho_p - \rho)}{\rho_p} + \vec{F} \tag{5}$$

Where $\vec{u}_p$ is the particle velocity, C_D is the drag coefficient, Re is the Reynolds number, ρ_p is the particle density and d_p is the particle diameter.

During the normal operation of the device, the most critical mechanisms considered are the wear and the erosion by particle impact. The overall correlation for the erosion rate, Eq. (6), has been established empirically [15, 16]:

$$E = m_p\, k\, C\, f(\alpha)\, V_p^n \tag{6}$$

Where E is the rate of the erosion (kg s-1), m_p is the particle flow (kg s-1), k is a material constant, C is a material constant that define the erosion resistance, $f(\alpha)$ is the impact function of the angle, V_p is the particle velocity and n is the velocity exponent, normally between 2.0 [16] or 2.5 [17] and 3.0. With low impact angles, $\alpha \leq 18.5°$, the particles collides the surface and remove a small piece of material; the maximum erosion occurs at $\alpha = 18.5°$. With collide angles higher than 18.5°, the particles rebound or accumulated in small craters that are produced at the surface.

The factor angle, $f(\alpha)$, was calculated in relation with Finnie [18, 19], where $f(\alpha \leq 18.5°) = sin2\alpha - 3sin^2\alpha$ and $f(\alpha > 18.5°) = \frac{1}{3}cos^2\alpha$, approximate its behavior to a piecewise-polynomial function (Fig. 3).

The erosion rate (kg m-2 s-1) on the wall is defined as [14]:

$$E_R = \sum_{p=1}^{Np} \frac{\dot{m}_p\, C(d_p) V_p^n}{A_f} \tag{7}$$

ISSN 2348 – 7968

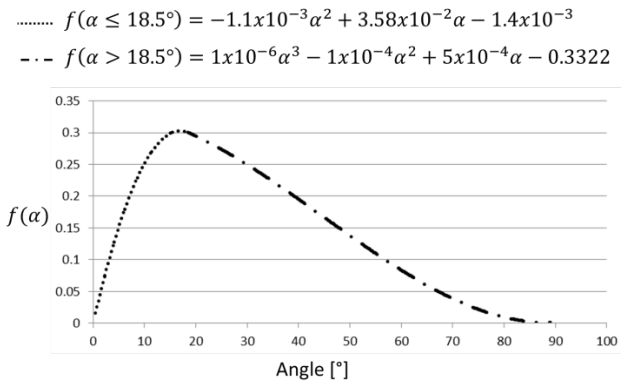

Fig. 3 Piecewise-polynomial Finnie's function.

Haugen et al. [16] and Keating - Nesic [18] recommend a value for $C(d_v) = 2x10^{-9}$ for steel eroded by sand. According to the literature, the value recommended is $C(d_v) = 1.8x10^{-9}$ and $n = 2.6$ as a default constant value for angular sand (200-250µm)/ carbon steel systems, $C(d_v) = 1x10^{-10}$ and $n = 2.6$ have been taken in this work in (7). The accretion rate is defined as [14]:

$$A_R = \sum_{p=1}^{Np} \frac{\dot{m}_p}{A_f} \qquad (8)$$

We can see that mathematical model (8) is part of the erosion expression, relating the flow of each discrete phase particles and the wall area in which the erosion study was conducted.

2.6 Boundary conditions

The boundaries I-1,I-2 and I-P (Fig. 1) are pressure inlet condition and the boundary O is given as pressure outlet condition. The discrete phase enters in the system by I-P.

3. Results and Discussion

During clinker process, the particles are in CO_2 atmosphere and a temperature of 1090 K. Note that the preheated material on these conditions is very oxidative to be removed violently from this extreme environment. So their physicochemical properties will not be representative in order to control the clinker quality.
When the device is inserted into the desired process point, the particles enter through the extraction tube and some collisions occur on the front wall. This effect slows down the particles and is subjected to an under action of the negative pressure obtained by the injected gas flow device. The flow analysis in this work is subject to erosion and the direction and position of the second injection of gas into the device for extracting, cooling, collection and reduced erosion of the exhaust tube during normal process operation. Figure 4 shows the results of potential damage due the erosion rate in ITT and ITC. Observe the erosion distribution effect of the tangential gas injection tube in ITT is higher than in ITC, due to high radius difference in the main tube.

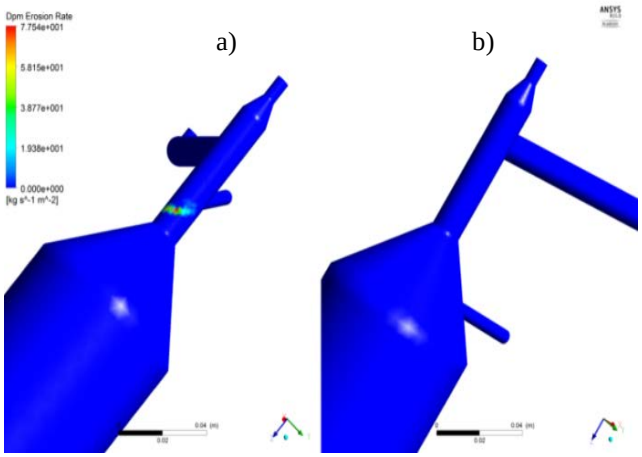

Fig. 4 Erosion rate in a) Inlet Tangential in main Tube (ITT), b) Inlet Tangential in Cone (ITC).

Figure 5 show a comparison of the inlet tubes (I-P) corresponding to the extracted samples ITT and ITC. Note on the ITT geometry the erosion distribution is inappreciable than the obtained in ITC. Such difference in the distributions of erosion that occurs at the input extraction tube (I-P) is due to the difference of flows that occur from injection way inlet gases.

ISSN 2348 – 7968

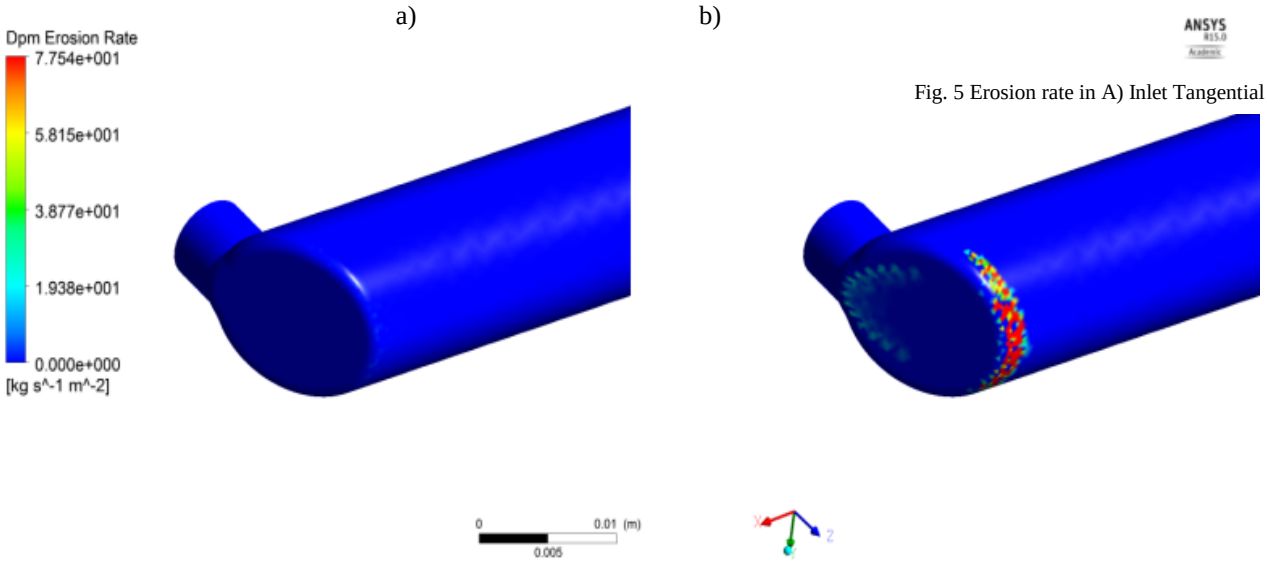

Fig. 5 Erosion rate in A) Inlet Tangential in main Tube (IT

In figure 6 the pressure distribution generated inside of this device is observed. The developments of pressures in the ITT geometry show the flow in the intersection of the extraction tube and the main tube (IET).

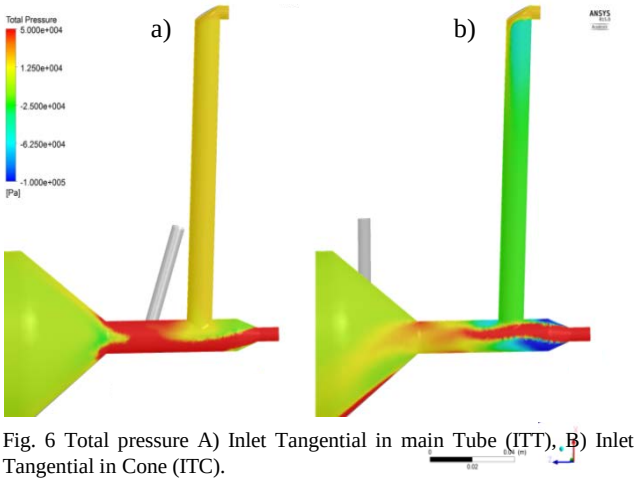

Fig. 6 Total pressure A) Inlet Tangential in main Tube (ITT), B) Inlet Tangential in Cone (ITC).

Note in the ITT case, above of IET the flow originates a kind of large wave, while the ITC this flow behavior is a ripple. This effect causes a slight perturbation in the generation of negative pressure which is used to extract the particles in I-P. This could explain the difference in the flow behavior of particles at the entrance of the extraction tube (see Fig.7)

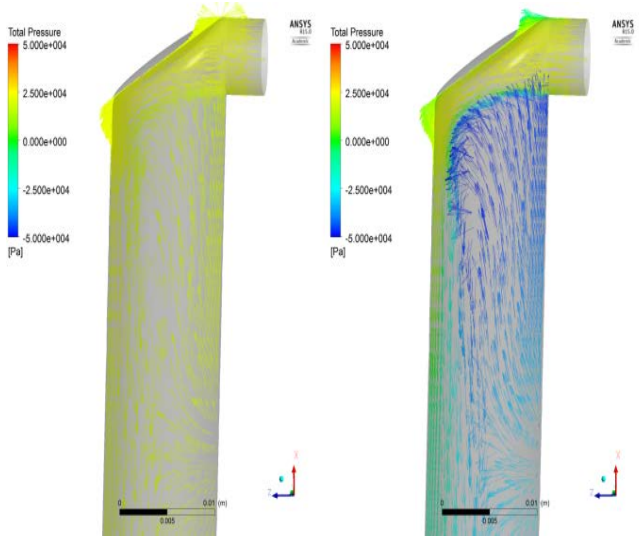

ISSN 2348 – 7968

Fig. 7 Vector field of total pressure in A) Inlet Tangential in main Tube (ITT), B) Inlet Tangential in Cone (ITC).

Table 1 summarizes the results of simulation analysis of this device. Note there is no significant difference regarding impacts number that occurs in the walls of the device. The difference could be observed only in the impacts number per unit area that occurring at a lower area in the ITT geometry than the ITC increasing the structural damage.

Regarding the extraction pressure generated by the device in the ITT is 0.207 MPa geometry and ITC of 0.187 MPa and contains a difference only of 0.02 MPa.

In the case of cooling effectiveness of the particles (Table 1 and figure 8), exhibit a temperature difference up to 1092.032 K to 301.29 K for ITT and 312.48 K to ITC geometries.

4. Conclusions

The new design sampling proposed, an extraction device for cement industry, was developed during this CFD design. The particles are extracted from a high-temperature atmosphere of CO_2, so that this condition is very oxidative to be removed violently from this extreme environment.

The results of potential damage by the erosion rate in ITT and ITC in which the effect of the erosion distribution of

Table 1: Results summary table of Inlet Tangential in main Tube, Inlet Tangential in Cone (ITC).

		ITT	ITC	Units
Surface Integral	Area weighted average.	0.0134569	0.014171486	Kg m-2 s-1
	Standard deviation	2.21888	36.1	Kg m-2 s-1
Gas pressure	Min	-207240.34	-187424.94	Pa
	Max	534635.38	507320.22	Pa
Particle temperature	Min	301.2905	312.4875	K
	Max	1092.032	1092.032	K

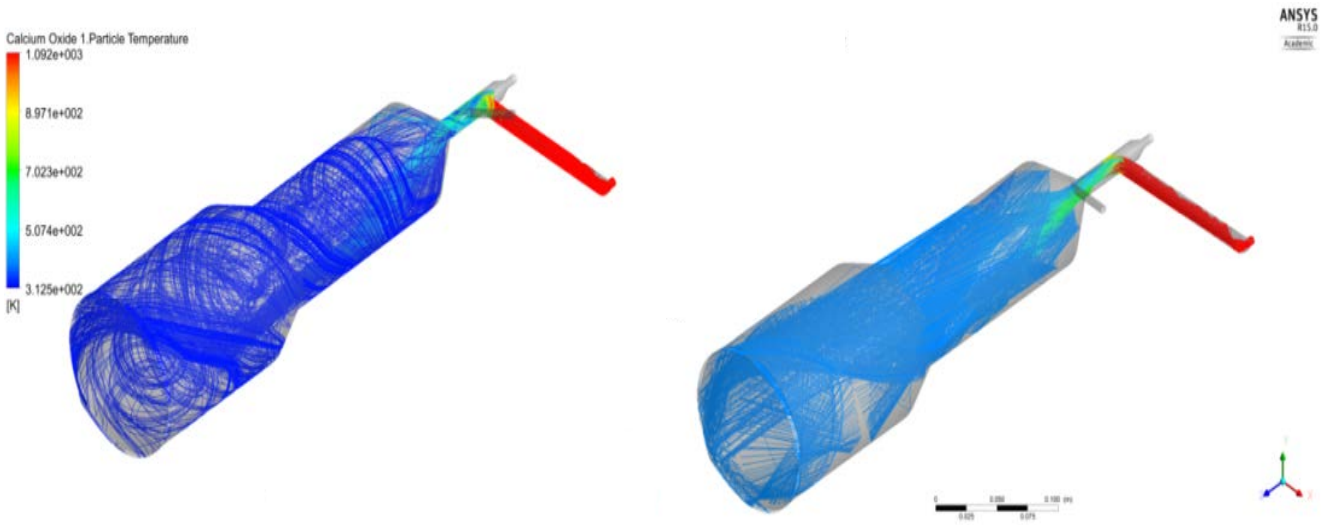

Fig. 8 Temperature distribution and particle trace in the geometry of A) Inlet Tangential in main Tube (ITT), B) Inlet Tangential in Cone (ITC).

ISSN 2348 – 7968

the injection tangential gas had a difference due to the trajectory radius. In this case, the flow is forced to follow a circumferential path.

Through CFD analysis could assess the damage caused by erosion. Due to a difference in turbulence above the intersection between the extraction tube and the main (IET), which where the negative pressure is generated by the gas injection. It was also possible to determine the influence of the input stream and in certain geometries generates this turbulence that could obstruct the exhaust duct or reduce its cycle life.

The number of impacts of the particles on the internal surface of the device there is no significant difference regarding the ITT and ITC. The only significate difference is ITT geometry, these impacts occurring at a lower area than the ITC increasing the structural damage.

The CFD analysis has demonstrated the utility of the model simulation. A good result is obtained for the new design comparing with the anterior results. Considering that best results will be obtained if a lighter material is evaluated with real time measurements in the industry.

Acknowledgments

Authors like thanks to the National Council of Science and Technology, CONACYT, México. Also are pleased to acknowledge to the Autonomus University of Juárez City, UACJ, Autonomus University of Chihuahua, UACH and Center for Advanced Materials Research, CIMAV.

References

[1] Y. Xie, K. Gao, J. Lan and G. Xie, “Computational Fluid Dynamics Modeling Three-Dimensional Unsteady Turbulent Flow and Excitation Force in Partial Admission Air Turbine”. Mathematical Problems in Engineering, 2013.

[2] Y. Xie, K. Lu, L. Liu, and G. Xie. “Fluid-Thermal-Structural Coupled Analysis of a Radial Inflow Micro Gas Turbine Using Computational Fluid Dynamics and Computational Solid Mechanics,” Mathematical Problems in Engineering, 2014

[3] Z.-j. Wang, J.-s. Zheng, L.-l Li, and S. Luo “Research on Three-Dimensional Unsteady Turbulent Flow in Multistage Centrifugal Pump and Performance Prediction Based on CFD,” Mathematical Problems in Engineering. 2013, http://dx.doi.org/10.1155/2013/589161

[4] X.-G. Song, J.-H. Park, S.-G. Kim, and Y.-C. Park ”Performance comparison and erosion prediction of jet pumps by using a numerical method,” Mathematical and Computer Modelling 57, 2013, pp 245-253

[5] I. Yimer, H. A. Becker, and E. Grandmaison, “The strong-jet/weak-jet problem: new experiments and CFD,” Combustion and flame 124(3), 2001, pp 481-502.

[6] A. Abdulaziz, “Performance and image analysis of a cavitating process in a small type venture Experimental,” Thermal and Fluid Science 53, 2014, pp 40-48.

[7] K. S. Mujumdar, and V. V. Ranade, “CFD modeling of rotary cement kilns,” Asia-Pacific Journal of Chemical Engineering 3(2), 2008, pp 106-118.

[8] H. Mikulčić, M. Vujanović, D. K. Fidaros, P. Priesching, I. Minić, R. Tatschl, N. Duić, and G. Stefanović, “The application of CFD modelling to support the reduction of CO2 emissions in cement industry,” Energy 45, 2012, 464-473.

[9] C. Huang, S. Chiovelli, P. Minev, J. Luo, and K. Nandakumar “A phenomenological model for erosion of materials in jet flow,” Powder Technology 187(3), 2008, pp 273-279.

[10] N. Kumar, and M. Shukla, “Finite element analysis of multi-particle impact on erosion in abrasive water jet machining of titanium alloy,” Journal of Computational and Applied Mathematics 236 (18), 2012, pp 4600-4610.

[11] L. Graham, D. Lester, and J. Wu, “Quantification of erosion distributions in complex geometries,” Wear 268 (9), 2010 , 1066-1071.

[12] H. A. López-Aguilar, J. A. Gómez, , A. Hernández, M. A. Merino, and A. P. Hernández, "Design and analysis of a sampling probe at high temperature under a CO2 atmosphere susceptible to oxidative damage. Part 1: Virtual design and dimensional optimization”, International Journal of Engineering and Innovative Technology 3(11), 2014, pp 245-249

[13] H. A. López-Aguilar, J. A. Gómez, , A. Hernández, M. A. Merino, and A. P. Hernández, "Design and analysis of a sampling probe at high temperature under a CO2 atmosphere susceptible to oxidative damage. Part 2: Optimization of operation." 3(11), 2014. pp. 262-266

[14] A. F. Ansys, Theory Guide. ANSYS inc. http://www.ansys.com, Accessed 20 October 2014.

[15] W. F. Adler, “Assessment of the State of Knowledge Pertaining to Solid Particle Erosion,” 1979 (Defense Technical Information Center Document).

[16] K. Haugen, O. Kvernvold, A. Ronold, and R. Sandberg, “Sand erosion of wear-resistant materials: Erosion in choke valves,” Wear 186, 1995, pp. 179-188.

[17]L. Nøkleberg, and T. Søntvedt, “Erosion of oil&gas industry choke valves using computational fluid dynamics and experiment,” International Journal of Heat and Fluid Flow 19 (6), 1998, pp. 636-643

[18] A. Keating, and S. Nesic, “Particle tracking and erosion prediction in three-dimensional bends,” Proc. of ASME FED Summer Meeting, 2000, pp. 11-15.

[19] I. Finnie, “Erosion of surfaces by solid particles,” Wear 3(2), 1960, pp. 87-103

Héctor Alfredo López Aguilar born January 24th 1980 in Uruapan Michoacán, México. Professional education: Master and PhD student in Environmental Science and Technology, Advanced Materials Research Center Chihuahua (CIMAV). Actually, the research activities are focused in combustion simulation, CFD and life cycle assessment methodology.

ISSN 2348 – 7968

Jorge Alberto Gómez, PhD in materials science.Born in Chihuahua,Chihuahua Mexico on July 3th 1974. Professional education: Industrial Engineer 2000, Technological Institute of Chihuahua. Master's and doctorate degree in materials science 2001 and 2008 respectively, CIMAV- Chihuahua. The relevant contributions in this subject is with the first paper "A Method to Evaluate the Tensile Strength and Stress–Strain Relationship of Carbon Nanofibers, Carbon Nanotubes, and C-chains" published in 2005 on SMALL, as several patents of nanomaterials devices. Actually, the research activities are focused in the lithography construction of the device, test "in situ" of carbon nanotubes employing the new device and study the mechanical properties of different types of carbons nanotubes as a different metallic catalyst on them. biography appears here. Degrees achieved followed by current employment are listed, plus any major academic achievements. Do not specify email address here.

Marco Antonio Merino Rodarte Professional education: Master student in Environmental Science and Technology, Advanced Materials Research Center Chihuahua (CIMAV).

Jose Alberto Duarte Moller, Ph. D. Born in Guaymas Sonora, Mexico on March the 27th, 1967. Professional education: B. Sc. Physics 1990, Physics Department, University of Sonora, Hermosillo Sonora, México,. M Sci. Physics of Materials 1993. Applied Physics Department, CICESE, Ensenada BC. Mexico, Ph D. Physics of Materials 1996. Applied Physics Department, CICESE, Ensenada BC. Mexico. Posdoctorate on Nanotechnology 2002, Chemistry Department University of Texas at El Paso, El Paso TX, USA. Actually works in the Center for Advanced Materials Research, CIMAV, Chihuahua,
Chih. Mexico

Antonino Pérez Hernández, PhD. Born in Gutierrez Zamora Veracruz, Mexico on January the 9th, 1963. Professional education: B. Sc. Physics 1987, Faculty of Physical and Mathematical Sciences, Autonomous University of Nuevo León, San Nicolás de los Garza Nuevo León, México. M Sci. in Mechanical Engineering with Specialization in Materials 1992, FIME-UANL, PhD Materials Engineering 1994, FIME-UANL. Dr. Pérez is actually member of the CIMAV. Relevant contributions; “Simulation of Flow Field Pattern Influence on the Hydrogen Consumption in A PEMFC” published in 2013 on Journal of New Materials for Electrochemical Systems. “The mathematical modeling of biomethane production and the growth of methanogenic bacteria in batch reactor systems fed with organic municipal solid waste” published in 2009 on Int. J. Global Warming. "A Method to Evaluate the Tensile Strength and Stress–Strain Relationship of Carbon Nanofibers, Carbon Nanotubes, and C-chains" published in 2005 on SMALL. Actually, the research activities: Applied Mathematics: Models of Physical Phenomena, Chemicals and Transfer. Process Simulation: Combustion, Filtration. Mass Transport Phenomena and Energy. Alternative Energy: Biomass, Bioelectricity, Hazardous Waste. Life Cycle Assessment (LCA).